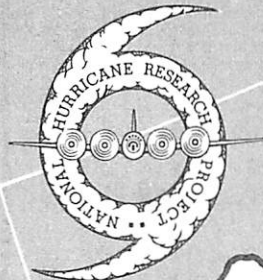


NATIONAL HURRICANE RESEARCH PROJECT

REPORT NO. 47

Concerning the Mechanics and
Thermodynamics of the Inflow Layer
of the Mature Hurricane



U. S. DEPARTMENT OF COMMERCE
Luther H. Hodges, Secretary
WEATHER BUREAU
F. W. Reichelderfer, Chief

NATIONAL HURRICANE RESEARCH PROJECT

REPORT NO. 47

Concerning the Mechanics and
Thermodynamics of the Inflow Layer
of the Mature Hurricane

by

Stanley L. Rosenthal

National Hurricane Research Project, Miami, Fla.



Washington, D. C.
September 1961

NATIONAL HURRICANE RESEARCH PROJECT REPORTS

Reports by Weather Bureau units, contractors, and cooperators working on the hurricane problem are preprinted in this series to facilitate immediate distribution of the information among the workers and other interested units. As this limited reproduction and distribution in this form do not constitute formal scientific publication, reference to a paper in the series should identify it as a preprinted report.

- No. 1. Objectives and basic design of the NHRP. March 1956.
- No. 2. Numerical weather prediction of hurricane motion. July 1956.
Supplement: Error analysis of prognostic 500-mb. maps made for numerical weather prediction of hurricane motion. March 1957.
- No. 3. Rainfall associated with hurricanes. July 1956.
- No. 4. Some problems involved in the study of storm surges. December 1956.
- No. 5. Survey of meteorological factors pertinent to reduction of loss of life and property in hurricane situations. March 1957.
- No. 6. A mean atmosphere for the West Indies area. May 1957.
- No. 7. An index of tide gages and tide gage records for the Atlantic and Gulf coasts of the United States. May 1957.
- No. 8. Part I. Hurricanes and the sea surface temperature field. Part II. The exchange of energy between the sea and the atmosphere in relation to hurricane behavior. June 1957.
- No. 9. Seasonal variations in the frequency of North Atlantic tropical cyclones related to the general circulation. July 1957.
- No. 10. Estimating central pressure of tropical cyclones from aircraft data. August 1957.
- No. 11. Instrumentation of National Hurricane Research Project aircraft. August 1957.
- No. 12. Studies of hurricane spiral bands as observed on radar. September 1957.
- No. 13. Mean soundings for the hurricane eye. September 1957.
- No. 14. On the maximum intensity of hurricanes. December 1957.
- No. 15. The three-dimensional wind structure around a tropical cyclone. January 1958.
- No. 16. Modification of hurricanes through cloud seeding. May 1958.
- No. 17. Analysis of tropical storm Frieda 1957. A preliminary report. June 1958.
- No. 18. The use of mean layer winds as a hurricane steering mechanism. June 1958.
- No. 19. Further examination of the balance of angular momentum in the mature hurricane. July 1958.
- No. 20. On the energetics of the mature hurricane and other rotating wind systems. July 1958.
- No. 21. Formation of tropical storms related to anomalies of the long-period mean circulation. September 1958.
- No. 22. On production of kinetic energy from condensation heating. October 1958.
- No. 23. Hurricane Audrey storm tide. October 1958.
- No. 24. Details of circulation in the high energy core of hurricane Carrie. November 1958.
- No. 25. Distribution of surface friction in hurricanes. November 1958.
- No. 26. A note on the origin of hurricane radar spiral bands and the echoes which form them. February 1959.
- No. 27. Proceedings of the Board of Review and Conference on Research Progress. March 1959.
- No. 28. A model hurricane plan for a coastal community. March 1959.
- No. 29. Exchange of heat, moisture, and momentum between hurricane Ella (1958) and its environment. April 1959.
- No. 30. Mean soundings for the Gulf of Mexico area. April 1959.
- No. 31. On the dynamics and energy transformations in steady-state hurricanes. August 1959.
- No. 32. An interim hurricane storm surge forecasting guide. August 1959.
- No. 33. Meteorological considerations pertinent to standard project hurricane, Atlantic and Gulf coasts of the United States. November 1959.
- No. 34. Filling and intensity changes in hurricanes over land. November 1959.
- No. 35. Wind and pressure fields in the stratosphere over the West Indies region in August 1958. December 1959.
- No. 36. Climatological aspects of intensity of typhoons. February 1960.
- No. 37. Unrest in the upper stratosphere over the Caribbean Sea during January 1960. April 1960.
- No. 38. On quantitative precipitation forecasting. August 1960.
- No. 39. Surface winds near the center of hurricanes (and other cyclones). September 1960.
- No. 40. On initiation of tropical depressions and convection in a conditionally unstable atmosphere. October 1960.
- No. 41. On the heat balance of the troposphere and water body of the Caribbean Sea. December 1960.
- No. 42. Climatology of 24-hour North Atlantic tropical cyclone movements. January 1961.
- No. 43. Prediction of movements and surface pressures of typhoon centers in the Far East by statistical methods. May 1961.
- No. 44. Marked changes in the characteristics of the eye of intense typhoons between the deepening and filling states. May 1961.
- No. 45. The occurrence of anomalous winds and their significance. June 1961.
- No. 46. Some aspects of hurricane Daisy, 1958. July 1961.

CONTENTS

	Page
ABSTRACT	1
1. INTRODUCTION	1
2. THE MECHANICAL EQUATIONS	1
Vertical advection term	2
Vertical integration	2
Tangential velocity solutions	5
Vorticity and divergence profiles	9
Pressure field	10
Kinetic energy considerations	15
3. HYDROSTATIC AND THERMODYNAMIC CONSIDERATIONS	17
Radial temperature gradient	17
Thermodynamic processes	18
Thermodynamic calculations	22
4. SUMMARY AND CONCLUSIONS	29
ACKNOWLEDGMENTS	29
REFERENCES	30

CONCERNING THE MECHANICS AND THERMODYNAMICS
OF THE INFLOW LAYER OF THE MATURE HURRICANE

Stanley L. Rosenthal
National Hurricane Research Project, Miami, Fla.

ABSTRACT

The Malkus-Riehl model of the hurricane inflow layer is extended to include vertical variations of radial velocity and density. The tangential equation of motion is solved to obtain radial distributions of tangential wind for certain specified inflow angles. The radial wind component is then obtained from the tangential wind and the inflow angle. The pressure profile is obtained from the radial equation of motion.

The thermodynamic constraints implied by these velocity and pressure fields are examined in relation to the vertical wind shear and the static stability. The diabatic heating and the various energy transformations needed to sustain the velocity and pressure fields are computed. The results appear to be quite reasonable.

1. INTRODUCTION

In the first part of this paper, the Malkus-Riehl [15] model of the hurricane inflow layer is extended to include vertical variations of radial motion and density. Velocity and pressure fields are obtained from the new version of the model. In the second part of the paper, an examination of the thermodynamics of the inflow layer is conducted and the energy transformations needed to sustain the model velocity and pressure fields are evaluated.

2. THE MECHANICAL EQUATIONS

Malkus and Riehl [15] assume the hurricane to be steady state and radially symmetric. They also neglect lateral mixing of momentum. These assumptions are retained here. However, during the course of this investigation, the author has become convinced that lateral mixing of momentum must be an extremely important mechanism for the maintenance of the hurricane eye. This problem will be treated in a subsequent paper.

Under the assumptions listed above, the equation of tangential motion (cylindrical coordinates, origin at the hurricane center) may be written

$$v_r \left(\frac{\partial v_\theta}{\partial r} + \frac{v_\theta}{r} + f \right) + w \frac{\partial v_\theta}{\partial z} = \frac{1}{\rho} \frac{\partial \tau_{\theta z}}{\partial z} . \quad (1)$$

$\tau_{\theta z}$ is the stress in the θ direction produced by vertical mixing of momentum. The remaining symbols are standard.

Vertical advection term. - In [15], the $w \frac{\partial v_{\theta}}{\partial z}$ term of equation (1) was neglected. This would appear to be justifiable. The calculations of E. S. Jordan [9] indicate that $|\frac{\partial v_{\theta}}{\partial z}|$ is less than 0.2 knots per 1000 feet in the lower 10,000 feet of the mean hurricane. This shear, of course, is not representative of the very lowest layer of the hurricane in which very large $|\frac{\partial v_{\theta}}{\partial z}|$ occur because of strong skin-friction effects. If we now take $w = 1 \text{ m. sec.}^{-1}$ for the storm core and $w = 5 \times 10^{-2} \text{ m. sec.}^{-1}$ for the outer portions of the storm,

$$\left| w \frac{\partial v_{\theta}}{\partial z} \right| \sim 3 \times 10^{-4} \text{ m. sec.}^{-2} \text{ (storm core)}$$

and

$$\left| w \frac{\partial v_{\theta}}{\partial z} \right| \sim 1.5 \times 10^{-5} \text{ m. sec.}^{-2} \text{ (outer portion)}$$

The sum of the remaining terms on the left-hand side of (1) may be written $v_r \zeta_a$ (ζ_a is the vertical component of the absolute vorticity). In the outer portion of a storm at 20° N.lat., ζ_a is on the order of $6 \times 10^{-5} \text{ sec.}^{-1}$ [9] and $|v_r|$ will be, say, 2 m. sec.^{-1} . Hence,

$$\left| v_r \zeta_a \right| \sim 1.2 \times 10^{-4} \text{ m. sec.}^{-2} \text{ (outer portion)}$$

In the storm core, a conservative estimate of ζ_a is $10^{-3} \text{ sec.}^{-1}$ [1, 12] and of $|v_r|$ at least 5 m. sec.^{-1} . From these figures,

$$\left| v_r \zeta_a \right| \sim 5 \times 10^{-3} \text{ m. sec.}^{-2} \text{ (storm core)}$$

Hence, within the inflow layer, $|v_r \zeta_a|$ would appear to be, on the average, at least ten times greater than $|w \frac{\partial v_{\theta}}{\partial z}|$. After the vertical advection term is dropped, equation (1) takes the form

$$\rho \zeta_a v_r = \frac{\partial \tau_{\theta z}}{\partial z} \quad (2)$$

Vertical integration. - Integration of (2) from $z = 0$ to the top of the inflow layer ($z = h$) yields

$$h (\overline{\rho v_r \zeta_a}) = \tau_{\theta h} - \tau_{\theta 0} \quad (3)$$

where

$$\overline{(\quad)} = \frac{1}{h} \int_0^h (\quad) dz. \quad (4)$$

The height origin, $z = 0$, is taken to be the "surface" in the usual meteorological sense. That is, $z = 0$ is a level several meters above mean sea level. In [15], and also here, $\tau_{\theta h}$ is neglected with respect to $\tau_{\theta 0}$. This is justified below.

$\tau_{\theta 0}$ is given by the empirical formula,

$$\tau_{\theta 0} = \rho_0 K_F V_0 v_{\theta 0} \quad (5)$$

K_F is the drag coefficient; V_0 is the wind speed at the surface; the remaining zero subscripts denote surface ($z = 0$) values. When an austausch assumption is made for $\tau_{\theta h}$, we obtain

$$\tau_{\theta h} - \tau_{\theta 0} = \left(K \frac{\partial v_{\theta}}{\partial z} \right)_{z=h} - \rho_0 K_F V_0 v_{\theta 0} \quad (6)$$

where K is the austausch coefficient. For $\left| (\partial v_{\theta} / \partial z)_{z=h} \right| = 0.2$ knots per 1000 feet and $K = 200 \text{ gram cm.}^{-1} \text{ sec.}^{-1}$, $\left| K (\partial v_{\theta} / \partial z)_{z=h} \right| \sim 6 \times 10^{-6} \text{ ton m.}^{-1} \text{ sec.}^{-2}$.

If we set K_F equal to the very small value of 1×10^{-3} , we find $\left| \rho_0 K_F V_0 v_{\theta 0} \right| \sim 10^{-6} \text{ ton m.}^{-3} \left| V_0 v_{\theta 0} \right|$. For V_0 of only 10 m. sec.^{-1} and for the very large inflow angle of 45° , $\left| \rho_0 K_F V_0 v_{\theta 0} \right| \sim 7 \times 10^{-5} \text{ ton m.}^{-1} \text{ sec.}^{-2}$. Provided that $K = 200 \text{ gram cm.}^{-1} \text{ sec.}^{-1}$ is a reasonable estimate of the austausch coefficient, we have

$$\tau_{\theta h} - \tau_{\theta 0} \approx - \tau_{\theta 0} \quad (7)$$

From equations (3), (5) and (7), we obtain

$$\frac{\tau_{\theta a}}{\rho v_r} = - \frac{\rho_0 K_F V_0 v_{\theta 0}}{h} \quad (8)$$

In the Malkus-Riehl [15] formulation, the vertical variations of all quantities contained in equation (8) were neglected. This approach allows equation (8) to be written

$$\frac{dv_{\theta}}{dr} = - f - v_{\theta} \left[\frac{1}{r} + \frac{K_F (v_{\theta}^2 + v_r^2)^{1/2}}{v_{rh}} \right] \quad (9)$$

However, from the Palmen-Riehl model [20], the calculations of Miller [17] and the calculations of Jordan [9], h is 3 to 4 km. In the normal tropical atmosphere [11], ρ varies by 26 percent over this depth. What is much more important is that v_r varies from values in excess of 20 knots [8] to zero. In our treatment of (8), v_r will be assumed to vary linearly with height. This,

of course, is only a rough approximation to the true vertical variation but it appears to be far better than a complete disregard of this effect. On the other hand, it seems reasonable, on the basis of [9], to neglect the vertical variation of v_θ at least to the extent that $\partial v_\theta / \partial z$ affects equation (8).

These assumptions allow us to write equation (8) in the form

$$\bar{\zeta}_a (\overline{\rho v_r}) = - \frac{\rho_0 K_F}{h} [\bar{v}_\theta^2 + 4\bar{v}_r^2]^{1/2} \bar{v}_\theta, \quad (10)$$

since

$$v_\theta \approx \bar{v}_\theta \approx v_{\theta 0}, \quad (11)$$

$$2\bar{v}_r \approx v_{r0} \quad (12)$$

and

$$v_r = 2\bar{v}_r (1 - z/h). \quad (13)$$

When the density of the mean tropical atmosphere [11] is plotted against height, one finds that the vertical variation over the lowest 4 km. departs very little from linearity. Therefore,

$$\rho = \rho_0 + bz \quad (14)$$

and

$$b = \frac{\rho_h - \rho_0}{h}. \quad (15)$$

From (13), (14) and (15), we obtain

$$\overline{\rho v_r} = \frac{1}{h} \int_0^h \rho v_r dz = \bar{\rho} \bar{v}_r + \frac{(\rho_0 - \rho_h)}{6} \bar{v}_r. \quad (16)$$

The second term on the right-hand side of (16) is less than 3 percent of $\bar{\rho} \bar{v}_r$ and will be neglected. Equation (10) may now be written

$$\bar{\zeta}_a = \frac{d \bar{v}_\theta}{dr} + \bar{v}_\theta / r + f = - \frac{\rho_0 K_F}{\bar{\rho} \bar{v}_r h} [\bar{v}_\theta^2 + 4\bar{v}_r^2]^{1/2} \bar{v}_\theta \quad (17)$$

or

$$\frac{d \bar{v}_\theta}{dr} = - \bar{v}_\theta \left\{ \frac{1}{r} - \frac{\rho_0 K_F}{\bar{\rho} h} \left[(\bar{v}_\theta / \bar{v}_r)^2 + 4 \right]^{1/2} \right\} - f. \quad (18)$$

To obtain (18), we have utilized the restriction, $\bar{v}_r < 0$.

Tangential velocity solutions. - To obtain solutions of (9), Malkus and

Riehl postulated the sine of the inflow angle $(v_r / (v_r^2 + v_0^2)^{1/2})$, in particular, they assumed this quantity to be constant for $100 \text{ km.} \leq r \leq 800 \text{ km.}$ and to vary in a linear fashion from $r = 100 \text{ km.}$ to $r = 25 \text{ km.}$ at which point the inflow angle was assumed to be zero. The outer portion of this relationship is taken from the Palmén-Riehl model [20]. The inner portion is more difficult to justify. Equation (9) shows that a maximum in the v_θ profile will occur only if the frictional term exceeds the total magnitude of the remaining terms over some range of r . This is possible only if the sine of the inflow angle becomes sufficiently small. Although not explicitly stated in [15], this may well have been the main justification for the selection of the inflow-angle relationship at $r \leq 100 \text{ km.}$

Malkus and Riehl set K_F/h equal to $1.36 \times 10^{-6} \text{ m.}^{-1}$ and obtained solutions of (9) for a series of outer inflow angles. With an inflow angle of 20° , the solution showed a maximum v_θ of approximately 58 m. sec.^{-1} . This is consistent with the Palmén-Riehl model [20]. With larger inflow angles, stronger maximum winds were obtained.

In this paper, we have obtained solutions to equation (18) by a procedure which is quite similar to that described above. That is, we have prescribed the radial distribution of the inflow angle of the vertically averaged wind. The Malkus-Riehl function was not used for two reasons: (1) It appeared desirable to utilize a function characterized by a continuous variation in the radial derivative of the inflow angle; (2) specification of the tangent of the inflow angle $(\bar{v}_r / \bar{v}_\theta)$ appeared to be more convenient than specification of the sine of this angle.

After some experimentation, the relationships

$$\bar{v}_r / \bar{v}_\theta = - \frac{I}{\exp \left\{ \frac{(b-a) \ln 2}{r-a} \right\}}, \quad r \geq a \quad (19)$$

and

$$\bar{v}_r / \bar{v}_\theta = 0, \quad r < a \quad (19a)$$

were selected. In (19), a and b are constants having the dimensions of lengths. I is a non-dimensional constant. The ratio $\bar{v}_r / \bar{v}_\theta$ vanishes at $r = a$ and is equal to $-I/2$ when $r = b$. At large values of r , $\bar{v}_r / \bar{v}_\theta \approx -I$.

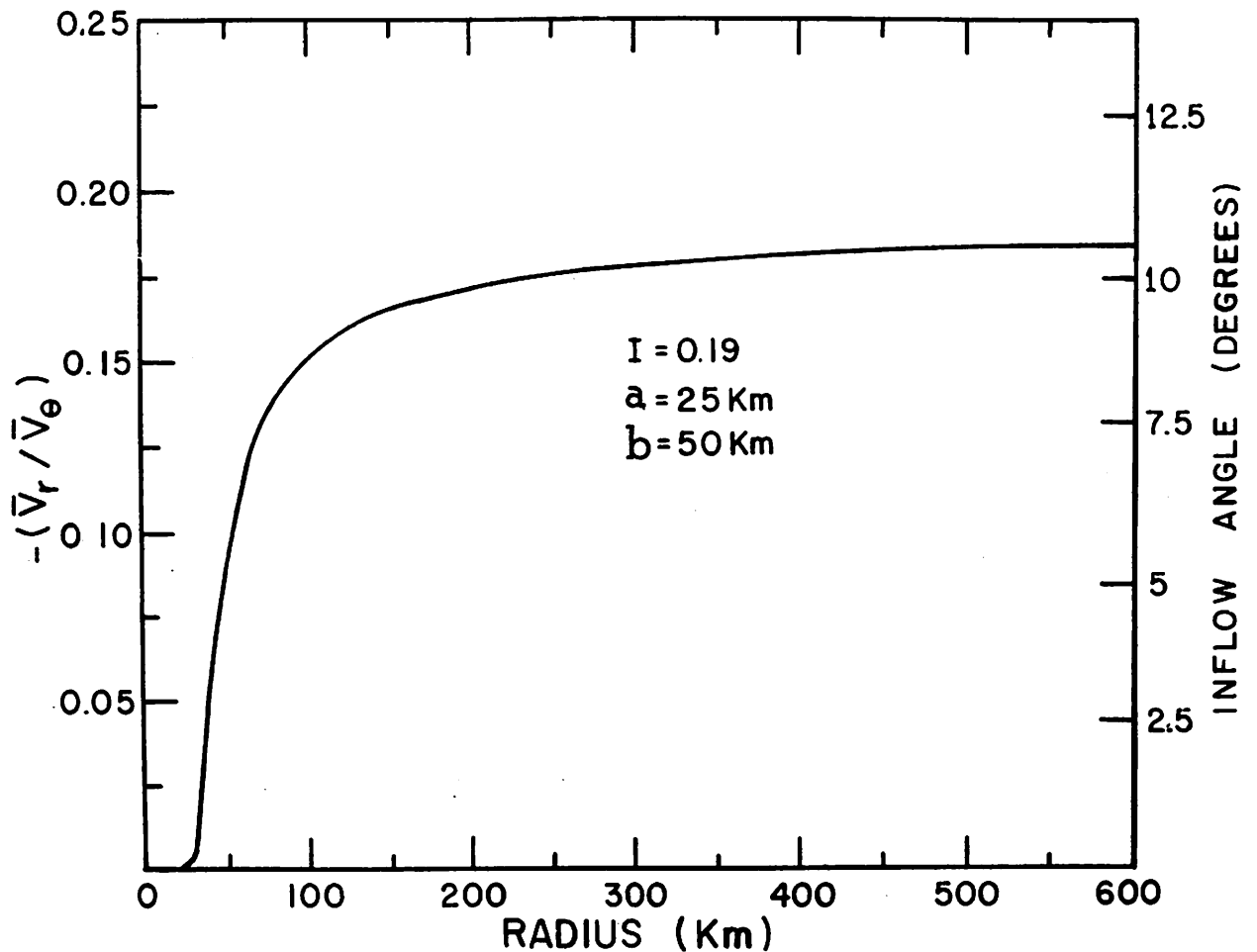


Figure 1. - Prescribed relationship between tangential and radial velocity components for $I = 0.19$, $a = 25$ km., $b = 50$ km.

Also,

$$\lim_{r \rightarrow a} \frac{d}{dr} \left(\frac{\bar{v}_r}{\bar{v}_\theta} \right) = 0. \quad (20)$$

For computational purposes, a and b were set equal to 25 and 50 km., respectively. A graph of (19), with $I = 0.19$, is illustrated by figure 1.

Substitution of (19) into (18) results in a first order, non-linear, ordinary differential equation for \bar{v}_θ . The resulting equation cannot be solved in closed form. Therefore, numerical solutions were obtained. To do this, it was necessary to assign values to ρ_0 , $\bar{\rho}$, K_F , h , I , and f . It has already been noted that [17] and [20] indicate h to be 3 to 4 km. We used $h = 3.5$ km. in our computations.

The studies of Deacon [3], Ekman [4], and Palmén and Laurila [19], as well as the surveys of Priestley [22] and Sverdrup [24], showed that $K_F = 2.4 \times 10^{-3}$ is a reasonable value for maritime winds of 30-40 knots. It also appears that smaller K_F apply to weaker winds and that virtually nothing is known about K_F for winds in excess of 30-40 knots. In view of this uncertainty, $K_F = 2.4 \times 10^{-3}$ was used at all wind speeds. Therefore, $K_F / h = 0.69 \times 10^{-6} \text{ m.}^{-1}$. This is about half of the value used by Malkus and Riehl.

Jordan's mean tropical atmosphere [11] was used to evaluate ρ_0 and $\bar{\rho}$. ρ_0 was taken to be $1.16 \times 10^{-3} \text{ ton m.}^{-3}$. $\bar{\rho}$ was obtained by vertical integration of (14) ($\bar{\rho} = [\rho_0 + \rho_h]/2$) with $\rho_h = 0.84 \times 10^{-3} \text{ ton m.}^{-3}$. This procedure gives $\bar{\rho} = 1.00 \times 10^{-3} \text{ ton m.}^{-3}$.

The parameter I was varied from solution to solution. Since $|v_r|$ decreases upward while v_θ , to a first approximation, is invariant with height in the inflow layer, $|v_r / v_\theta|$ must decrease with height. In view of the assumed linearity of v_r , $|\bar{v}_r / v_\theta|$ will be about one-half of $|v_{r0} / v_{\theta 0}|$. If the surface inflow angle at large r is to be, say, 20° (corresponding to one of the Malkus-Riehl cases), the inflow angle for the vertically integrated winds should be about 10° . This reasoning provides a basis for the selection of I. Finally, we used $f = 5 \times 10^{-5} \text{ sec.}^{-1}$ which is valid for 20° N. lat.

Equations (18) and (19) were solved simultaneously by means of Milne's method [18]. The IBM 650 at the National Hurricane Research Project was used for these computations. Truncation error was checked at each grid point and whenever a preset value was exceeded, the radial increment was reduced by a factor of 1/2 and the computation was continued with the new increment. For the calculations reported on below, the maximum truncation error was set at $10^{-2} \text{ m. sec.}^{-1}$ and the initial radial increment (Δr) was 10 km. v_θ was set equal to 10 m. sec.^{-1} at $r = 600 \text{ km.}$ For each solution, the machine retained $\Delta r = 10 \text{ km.}$ until $r = 100 \text{ km.}$ was reached. At radii smaller than 100 km., the machine frequently reduced Δr . In all runs, Δr became as small as 10 m. in the vicinity of $r = 27 \text{ km.}$ When this occurred, the computation was terminated on the basis of machine-time considerations.

Figure 2 shows the \bar{v}_θ profiles for $I = 0.19, 0.25,$ and 0.30 (inflow angles of $10.7^\circ, 14.0^\circ,$ and 16.7° at $r = \infty$, respectively). The \bar{v}_θ increase as I becomes larger as in the case of the Malkus-Riehl model [15]. Some of the basic features of figure 2 are summarized in table 1.

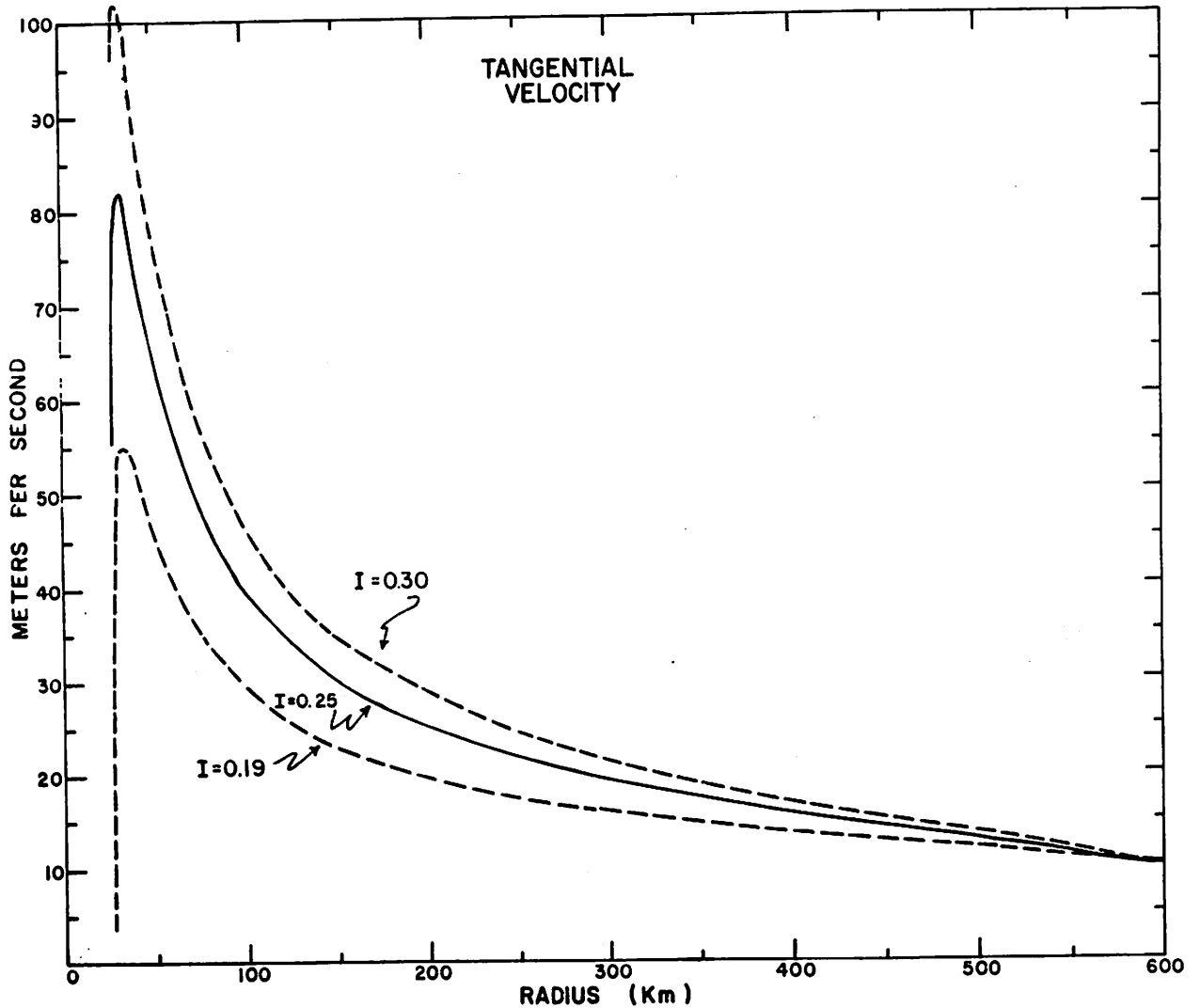


Figure 2. - Theoretical tangential velocity profiles for inflow angles at $r = \infty$ of 10.7° ($I = 0.19$), 14° ($I = 0.25$), and 16.7° ($I = 0.30$).

Table 1. - Summary of \bar{v}_θ solutions.

I	Inflow angle at $r = \infty$	Maximum \bar{v}_θ (m. sec. ⁻¹)	Radius of maximum \bar{v}_θ
0.19	10.7°	55	33.8 km.
0.25	14.0°	82	32.5 km.
0.30	16.7°	102	32.0 km.

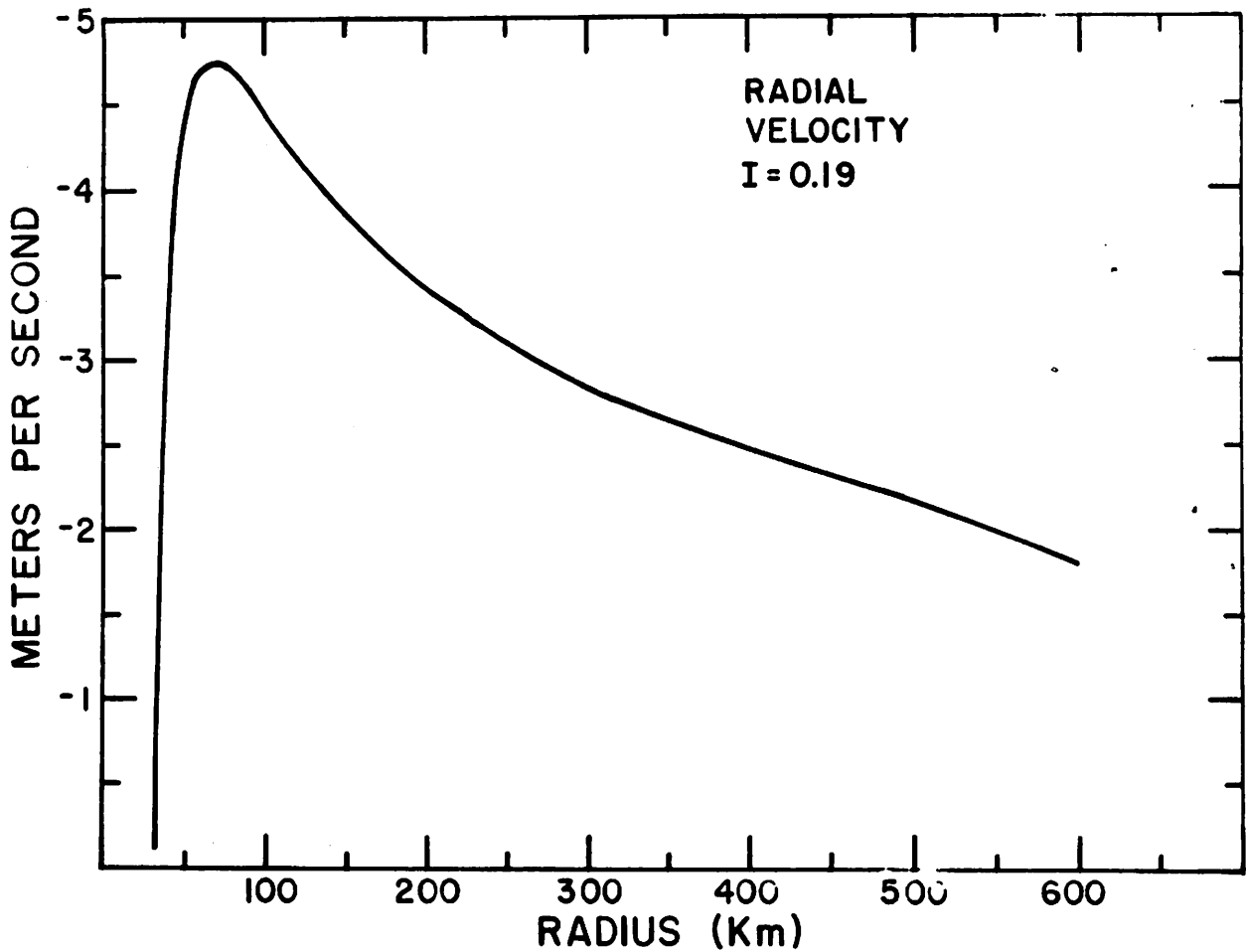


Figure 3. - Theoretical radial velocity profile for an inflow angle of 10.7° ($I = 0.19$) at $r = \infty$.

It will be noted that the shapes of the profiles agree quite well with those found by LaSeur [12] and Blumen and LaSeur [1] for hurricanes Ione and Edith and by Colón [2] for hurricane Daisy. In particular, the model and observations agree that intense winds are to be found only in a very narrow zone surrounding the radius of maximum v_θ . The extremely rapid decrease of \bar{v}_θ inward from the maximum value does not appear to be excessive (see, for instance, [2, 12]).

Figure 3 shows the radial profile of \bar{v}_r ($I = 0.19$). In the literature, one finds considerable disagreement concerning the nature of the hurricane radial velocity profile. In view of this uncertainty, one must conclude that v_r profiles probably vary markedly from one hurricane to another and that the reality of figure 3 cannot be judged at this time.

Vorticity and divergence profiles. - Equation (18) was solved for the mean relative vorticity ($\bar{\zeta}$),

$$\bar{\zeta} = \frac{d\bar{v}_\theta}{dr} + \frac{\bar{v}_\theta}{r}. \quad (21)$$

$\bar{\zeta}$ values (for $I = 0.19$) are shown by figures 4 and 5. We note that $\bar{\zeta}$ varies from small negative values at $r = 600$ km. to values in excess of $3 \times 10^{-2} \text{ sec.}^{-1}$ close to $r = 28$ km. At radii greater than 100 km., the agreement with the vorticities presented by Hughes [8] is fairly good. The theoretical values are, however, somewhat smaller than the empirical ones. In this same region ($r > 100$ km.), the theoretical vorticities are also somewhat smaller than the values given by Miller's data [17]. Again, however, the shape of the theoretical profile agrees fairly well with that of the empirical profile. Better correspondence between theoretical and observed vorticities is found when comparisons are made with E. Jordan's data [9]. However, these data do not extend inward of $r = 220$ km.

Figure 5 shows the theoretical distribution of $\bar{\zeta}$ (on a semilogarithmic graph) at $r \leq 60$ km. This distribution of $\bar{\zeta}$, even with regard to magnitude, agrees quite well with the core-vorticity distributions obtained by LaSeur [12] and Blumen and LaSeur [1] for hurricane Ione and by Colón [2] for hurricane Daisy.

The radial derivative of \bar{v}_r may be obtained by differentiation of equation (19). The resulting equation, together with equations (18) and (19), may be used to compute the mean divergence (\bar{D}),

$$\bar{D} = \frac{d\bar{v}_r}{dr} + \frac{\bar{v}_r}{r}. \quad (22)$$

The \bar{D} profile ($I = 0.19$) is shown in figure 4. These are consistent with Hughes' data [8], the Palmén-Riehl model [20], and the computations of Blumen and LaSeur [1] and LaSeur [12] to the extent that all strong divergences are concentrated in a narrow ring close to the maximum winds.

Pressure field. - The pressure profiles, needed to maintain these velocity fields, may now be obtained. The radial equation of motion is

$$v_r \frac{\partial v_r}{\partial r} + w \frac{\partial v_r}{\partial z} - \frac{v_\theta^2}{r} - fv_\theta - \frac{1}{\rho} \frac{\partial \tau_{rz}}{\partial z} = - \frac{1}{\rho} \frac{\partial p}{\partial r} \quad (23)$$

τ_{rz} is the stress in the radial direction produced by vertical mixing of momentum. The remaining symbols are as defined previously. Examination of our \bar{v}_r and \bar{D} profiles indicated that the advective terms of (23) are each 5-10 percent of the Coriolis term at relatively large distances from the radius of maximum winds. Furthermore, in this outer region, the two advective terms have opposite signs and tend to leave a very small residual. Close to the radius of maximum winds, the advective terms are quite small compared to the centrifugal term. Hence, neglect of the $v_r (\partial v_r / \partial r)$ and $w (\partial v_r / \partial z)$ terms is entirely reasonable for the purpose of computing the pressure field. When the advective terms are dropped and (23) is integrated over the depth of the inflow layer, one obtains

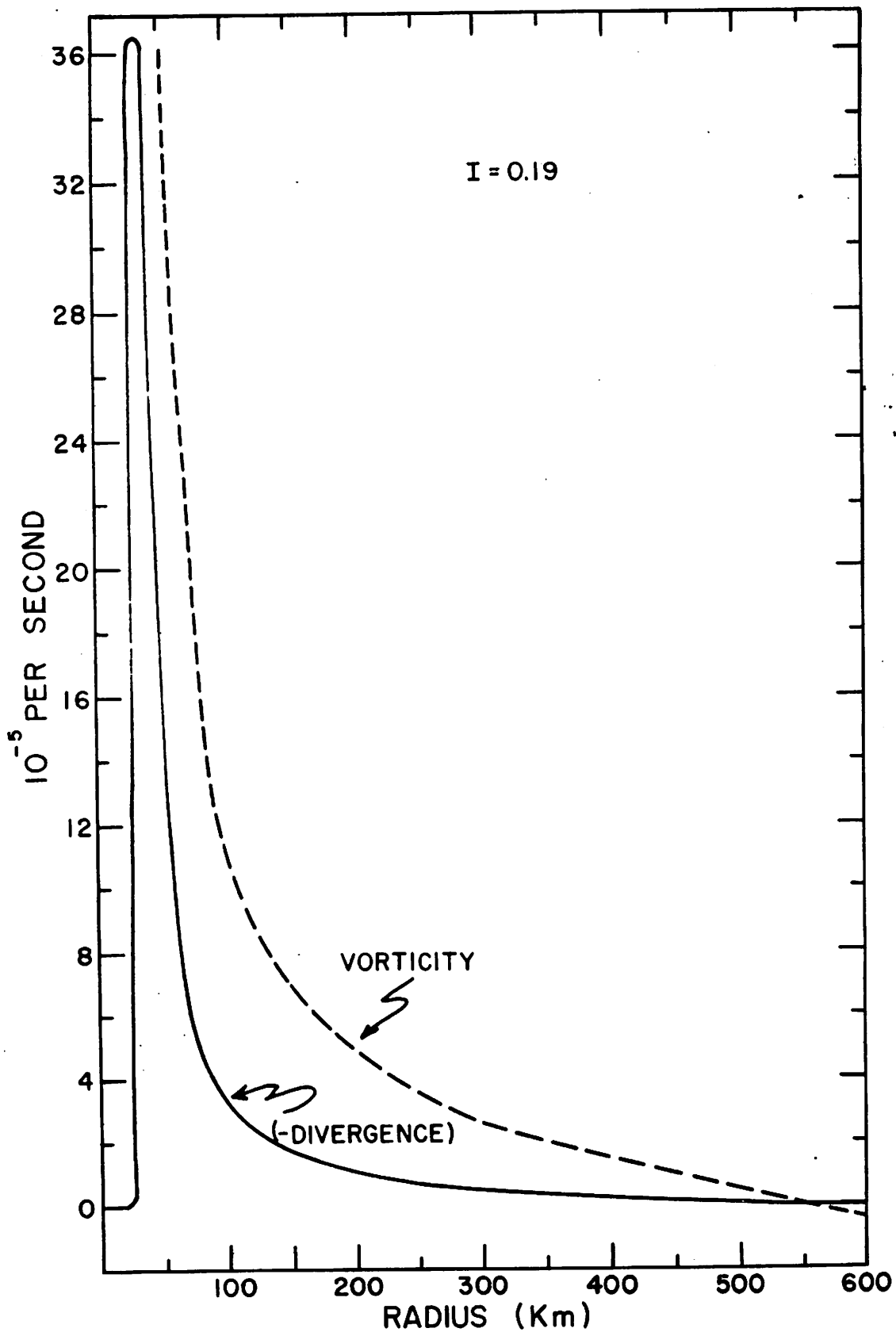


Figure 4. - Theoretical profiles of divergence and relative vorticity for an inflow angle of 10.7° ($I = 0.19$) at $r = \infty$.

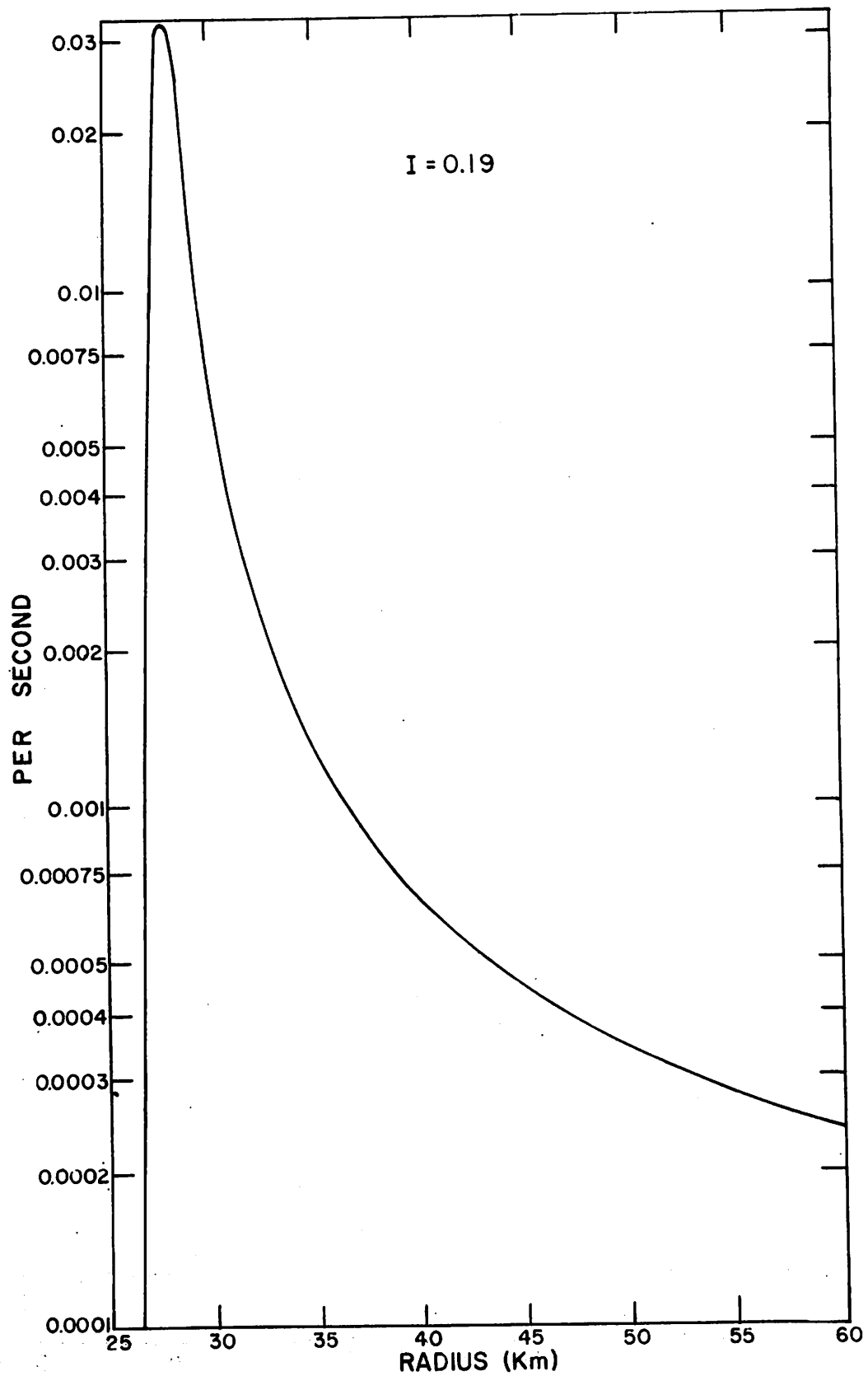


Figure 5. - Theoretical profile of relative vorticity for $r \leq 60$ km. when the inflow angle at $r = \infty$ is 10.7° ($I = 0.19$).

$$-\bar{p} \left(\frac{\bar{v}_\theta^2}{r} + f \bar{v}_\theta \right) - \frac{(\tau_{rh} - \tau_{r0})}{h} = - \frac{\partial \bar{p}}{\partial r}. \quad (24)$$

We have again neglected the vertical variation of v_θ . τ_{rh} would appear to be quite small when compared with τ_{r0} . The computations of Jordan [9] and the Palmén-Riehl model [20] indicate that $\partial v_r / \partial z$ and v_r approach zero simultaneously as z approaches h . With an Austausch assumption,

$$\tau_{rh} \propto \left(\frac{\partial v_r}{\partial z} \right)_{z=h} \approx 0.$$

Hence,

$$\tau_{rh} - \tau_{r0} \approx - \tau_{r0} = - \rho_0 K_F V_0 v_{r0} \quad (25)$$

With the aid of (25), equation (24) may be written

$$\frac{\partial \bar{p}}{\partial r} = \bar{p} \left(\frac{\bar{v}_\theta^2}{r} + f \bar{v}_\theta \right) - \frac{2\rho_0 K_F}{h} (\bar{v}_\theta^2 + 4\bar{v}_r^2)^{1/2} \bar{v}_r. \quad (26)$$

Equation (26) was integrated for the $I = 0.19$ case by means of the trapezoidal rule. \bar{p} at $r = 600$ km. was set equal to 833 mb. This is the $z = 1.75$ km. pressure in Jordan's mean tropical atmosphere [11]. Although the pressure at 1.75 km. is only an approximation to \bar{p} , a plot of the pressure-height curve for the lowest 3.5 km. will quickly convince the reader that the approximation is fairly good.

Figure 6 indicates that the central \bar{p} is 795 mb. and that the \bar{p} difference between the storm center and the outer periphery of the storm is 38 mb. That this is a reasonable pressure configuration for a storm with maximum winds of around 110 knots may be verified by reference to hurricane Daisy [2] which had wind speeds in the lower layers nearly equal to those found in the model. Fletcher's empirical relationship [5]

$$V_{OM} = 16 (p_{OR} - p_{OC})^{1/2} \quad (27)$$

may also be used to examine the reality of the model pressure field. In (27), V_{OM} is the maximum wind speed (knots) at $z = 0$ and p_{OR} and p_{OC} are, respectively, the storm's peripheral and central pressures (millibars) at $z = 0$. V_{OM} for the model storm is about 110 knots. Equation (27) gives

$$(p_{OR} - p_{OC}) = 48 \text{ mb.} \quad (28)$$

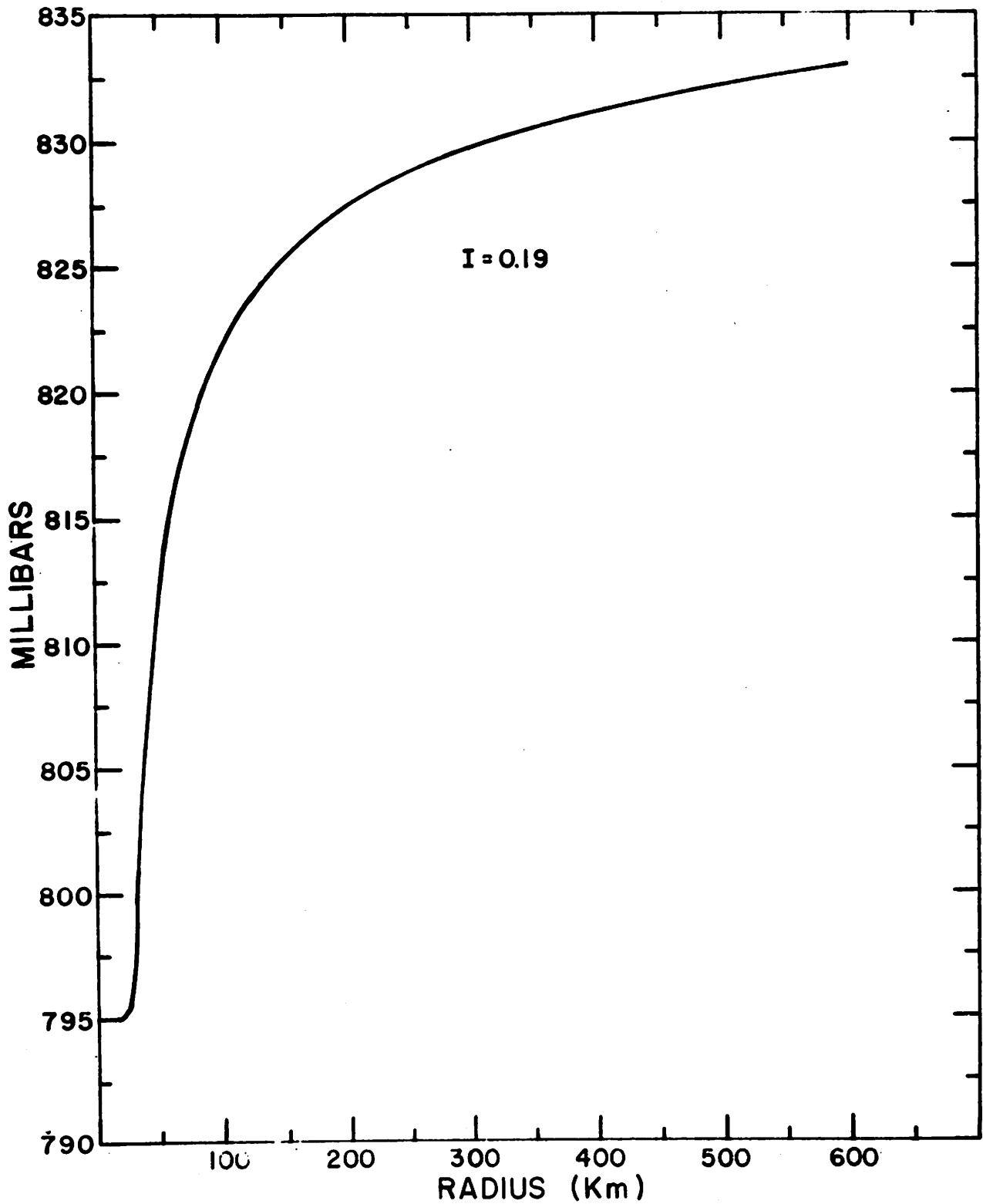


Figure 6. - Theoretical pressure profile at $z = 1.75$ km. when the inflow angle at $r = \infty$ is 10.7° ($I = 0.19$).

The value given by (28) must be reduced by about 15 percent for comparison with the \bar{p} configuration because of the increase of specific volume between $z = 0$ and $z = 1.75$ km. When this is done, we obtain $(p_{OR} - p_{OC}) = 41$ mb. which is only 3 mb. greater than the corresponding difference in the model pressures.

Kinetic energy considerations. - The equation of horizontal motion may be written

$$D\mathbf{V} / Dt = -f \hat{k} \times \mathbf{V} - \frac{1}{\rho} \nabla p + \mathbf{F} \quad (29)$$

where \mathbf{V} is the horizontal wind vector, \hat{k} is a unit vertical vector, \mathbf{F} is the frictional force per unit mass, D/Dt is the substantial time derivative, and ∇ is the horizontal del operator. Scalar multiplication of equation (29) by \mathbf{V} yields

$$DK/Dt = -1/\rho \mathbf{V} \cdot \nabla p + \mathbf{V} \cdot \mathbf{F}. \quad (30)$$

$K = (\mathbf{V} \cdot \mathbf{V})/2$ (the specific kinetic energy). The terms on the right-hand side of (30) are usually interpreted [21] as follows: $-(1/\rho) \mathbf{V} \cdot \nabla p$ is the rate at which specific enthalpy and specific potential energy are converted to specific kinetic energy following a parcel; $\mathbf{V} \cdot \mathbf{F}$ is the rate at which the specific kinetic energy of a parcel is dissipated by friction.

Within the framework of our model, \mathbf{F} at $z = 1.75$ km. is given by

$$\mathbf{F} = - \left[\frac{\rho_0 K_F}{\bar{\rho} h} \right] [4 \bar{v}_r^2 + \bar{v}_\theta^2]^{1/2} [\bar{v}_\theta \hat{\theta} + \bar{v}_r \hat{r}]. \quad (31)$$

$\hat{\theta}$ and \hat{r} are, respectively, unit vectors in the θ and r directions. Equation (31) may be verified by inspection of (11) and (26) with cognizance of the fact that \bar{v}_θ and \bar{v}_r are, in the model, the actual winds at $z = 1.75$ km. The rate of dissipation of specific kinetic energy for parcels at $z = 1.75$ km. is then given by

$$\mathbf{V} \cdot \mathbf{F} = - \left[\frac{\rho_0 K_F}{\bar{\rho} h} \right] [4 \bar{v}_r^2 + \bar{v}_\theta^2]^{1/2} [\bar{v}_\theta^2 + \bar{v}_r^2]. \quad (32)$$

The rate of production of specific kinetic energy for parcels at this level is given by

$$-1/\rho \mathbf{V} \cdot \nabla p = -(\bar{v}_r / \bar{\rho}) (\partial \bar{p} / \partial r) \quad (32a)$$

if it is assumed that $(1/\bar{\rho})(\partial \bar{p} / \partial r)$ may be written for the $z = 1.75$ km. value of $(1/\rho)(\partial p/\partial r)$. The radial distribution of the ratio

$$\frac{\mathbf{V} \cdot \mathbf{F}}{-\frac{1}{\rho} \mathbf{V} \cdot \nabla p}$$

for the $I = 0.19$ case is given by table 2. ($-\frac{1}{\rho} \mathbf{V} \cdot \nabla p$, itself, is discussed in more detail in later sections of this paper; its radial profile for the $I = 0.19$ case is illustrated by fig. 10).

Perhaps the most significant feature of table 2 is the result that $\mathbf{V} \cdot \mathbf{F}$ exceeds $-\frac{1}{\rho} \mathbf{V} \cdot \nabla p$ in a ring close to the storm center. A similar result was obtained by Palmén and Riehl [20]. However, their dissipation and production rates were evaluated for the integrated effect of the entire troposphere. Since we are working with rates per unit mass following a parcel, a direct comparison between our numerical values and those obtained in [20] is not possible. Qualitatively, the results of [20] show the dissipation rate to exceed the production rate over the ring which extends from $r = 2^\circ$ lat. to $r = 0.25^\circ$ lat. Our results show the region in which

Table 2. - Ratio of the rate of frictional dissipation of specific kinetic energy ($\mathbf{V} \cdot \mathbf{F}$) to the rate of production of specific kinetic energy (S) at $z = 1.75$ km. for $I = 0.19$

Radius (km.)	$(\mathbf{V} \cdot \mathbf{F})/S$
500	0.76
400	0.78
300	0.75
200	0.67
100	0.48
80	0.44
60	0.40
50	0.41
40	0.52
35	0.81
33.75	1.00
32.5	1.34
30.0	3.92
29.5	5.87
29.0	9.12
28.5	15.9
28.0	37.8
27.5	97.9
27.3	129
27.1	65
27.0	12.4
26.9	1.5
26.87	1.00

$\nabla \cdot \mathbf{F} / - (1/\rho) \nabla \cdot \nabla p > 1$ to be the very narrow ring 26.87 km. $\leq r \leq 33.75$ km. If, for a moment, we confine our attention to the space volume delineated by this ring, we find that a steady-state velocity field can be maintained only if advection is sufficient to import kinetic energy at a rate equal to the difference in the per volume rates of kinetic energy production and dissipation. This has also been pointed out by Palmén [21]. Over the remainder of the storm, the production rate of kinetic energy exceeds the dissipation rate. In these regions, there must be an advective export of kinetic energy in order that steady conditions be maintained.

3. HYDROSTATIC AND THERMODYNAMIC CONSIDERATIONS

Radial temperature gradient. - An expression for the radial temperature gradient may be obtained through vertical differentiation of the pressure-gradient force per unit mass ($- [1/\rho] [\partial p/\partial r]$), introduction of the ideal gas law, and utilization of the hydrostatic equation. This procedure yields

$$\frac{\partial T}{\partial r} = \frac{T}{g} \left[\frac{\partial}{\partial z} \left(\frac{1}{\rho} \frac{\partial p}{\partial r} \right) + \frac{\gamma}{\rho T} \frac{\partial p}{\partial r} \right]. \quad (33)$$

$\gamma = -(\partial T/\partial z)$ is the lapse rate and g is the acceleration of gravity. Vertical differentiation of equation (23) (after dropping the advection terms) yields

$$\frac{\partial}{\partial z} \left(\frac{1}{\rho} \frac{\partial p}{\partial r} \right) = \frac{\partial v_{\theta}}{\partial z} \left(f + \frac{2v_{\theta}}{r} \right) + \frac{\partial}{\partial z} \left(\frac{1}{\rho} \frac{\partial \tau_{rz}}{\partial z} \right). \quad (34)$$

Elimination of $(\partial/\partial z)([1/\rho][\partial p/\partial r])$ between (33) and (34) produces the relationship

$$\frac{\partial T}{\partial r} = \frac{T}{g} \left(\frac{\partial v_{\theta}}{\partial z} \left(f + \frac{2v_{\theta}}{r} \right) \right) + \frac{T}{g} \frac{\partial}{\partial z} \left(\frac{1}{\rho} \frac{\partial \tau_{rz}}{\partial z} \right) + \frac{\gamma}{\rho g} \frac{\partial p}{\partial r}. \quad (35)$$

The term $\frac{T}{g} \frac{\partial}{\partial z} \left(\frac{1}{\rho} \frac{\partial \tau_{rz}}{\partial z} \right)$ will be neglected. A qualitative assessment of the effect produced by dropping this term may be obtained by a determination of its sign. In the inflow layer, where v_r is negative, $(1/\rho)(\partial \tau_{rz} / \partial z)$ should be positive. In view of the fact that v_r becomes less negative with height ($[\partial v_r / \partial z] > 0$), we would expect $\frac{\partial}{\partial z} \left(\frac{1}{\rho} \frac{\partial \tau_{rz}}{\partial z} \right)$ to be negative. Hence, by dropping this term, we underestimate the warm core characteristics of the storm.

Evaluation of (35) at $z = 1.75$ km. with the assumption $\frac{1}{\rho} \frac{\partial p}{\partial r} = \frac{1}{\rho} \frac{\partial \bar{p}}{\partial r}$, gives

$$\frac{\partial T}{\partial r} = \frac{T}{g} \frac{\partial v_{\theta}}{\partial z} \left(f + \frac{2\bar{v}_{\theta}}{r} \right) + \frac{\gamma}{g} \frac{1}{\rho} \frac{\partial \bar{p}}{\partial r} \quad (36)$$

Equation (36) was used to obtain temperature profiles for three different values of $\partial v_\theta / \partial z$. \bar{v}_θ and $(1/\rho)(\partial \bar{p} / \partial r)$ for $I = 0.19$ were used in these computations. The lapse rate, δ , was assumed to be pseudoadiabatic which is reasonable above the cloud base of the inflow layer [23]. The pseudoadiabatic lapse rate (Γ_s) is given by (see, for instance, [7])

$$\Gamma_s = \frac{g}{c_p} \left[\frac{1 + \frac{\epsilon L e_s}{p R T}}{1 + \frac{\epsilon L}{c_p p} \frac{de_s}{dT}} \right]. \quad (37)$$

c_p is the specific heat capacity at constant pressure for dry air, ϵ is the ratio of the molecular weight of water to that of dry air, L is the latent heat of vaporization for water, R is the individual gas constant for dry air, e_s is the equilibrium pressure for the vapor to liquid phase change of water.

e_s and de_s / dT were evaluated by means of the Clausius-Clapeyron equation. To carry out the numerical integration of (36), the temperature at $r = 560$ km. was set equal to the $z = 1.75$ km. temperature of Jordan's mean tropical atmosphere [11]. This value is 290° K. It should be noted that the model exhibits positive divergence at $r > 560$ km. and hence, the $\delta = \Gamma_s$ assumption is not valid when $r > 560$ km.

The temperature profiles obtained by integration of (36) are illustrated by figure 7. The various profiles are labeled with the values of $\partial v_\theta / \partial z$ used to obtain them. For purposes of orientation, $1.5 \times 10^{-4} \text{ sec.}^{-1}$ is roughly equal to a shear of 0.3 knots per kilometer.

All three cases are warm core when viewed from a constant pressure surface ($\partial T / \partial r$ on a constant pressure surface may be obtained by dropping the second term on the right-hand side of (36)). On level surfaces, however, distinct warm core characteristics are only to be found with large values of $\partial v_\theta / \partial z$; $\partial v_\theta / \partial z = -4.5 \times 10^{-4} \text{ sec.}^{-1}$ is quite a bit larger in magnitude than the average inflow-layer value of this shear [9]. For the two smaller shears, the storm is cold core on level surfaces. This result (lack of a distinct warm core) is not as unrealistic as one might, at first glance, conclude. Colón [2] has found distinct cold pockets at small radii in hurricane Daisy. These cold pockets were even evident on constant pressure surfaces. Many workers (see, for example, [10, 14, 23]) have noted that $\partial T / \partial r$ is relatively small within the inflow layer and that marked warm core characteristics are only to be found in the higher troposphere.

Thermodynamic processes. - The first law of thermodynamics, written for the ascent of saturated air, can be put into the form

$$\frac{DH}{Dt} = c_p \frac{DT}{Dt} - \frac{1}{\rho} \frac{Dp}{Dt} + L \frac{Dq_s}{Dt} \quad (38)$$

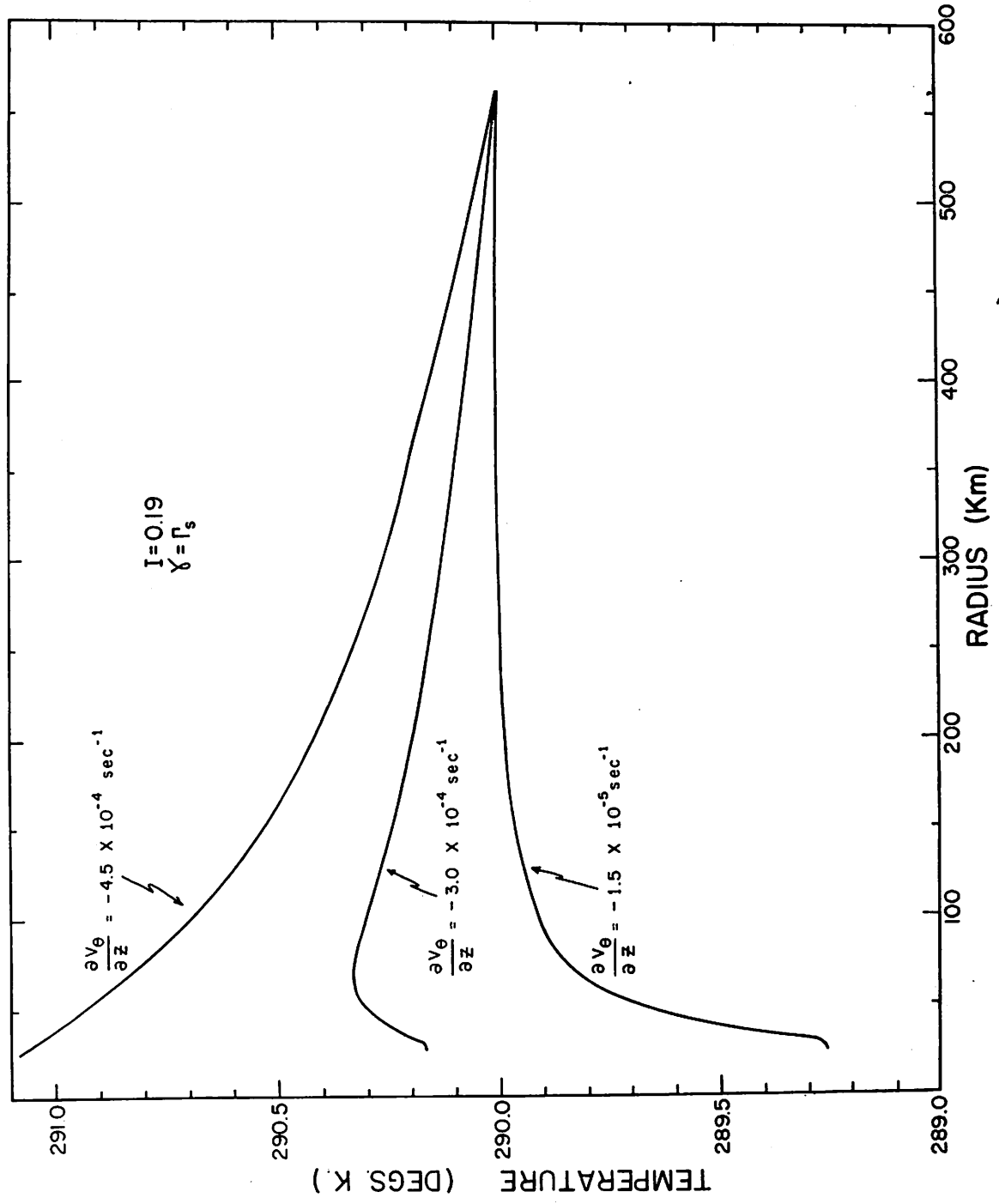


Figure 7. - Theoretical temperature profiles at $z = 1.75$ km. when the inflow angle at $r = \infty$ is 10.7° ($I = 0.19$) and $\partial V_\theta / \partial z$ is -4.5×10^{-4} , -3.0×10^{-4} , and $-1.5 \times 10^{-5} \text{ sec}^{-1}$

q_s is the saturation specific humidity. $\frac{DH}{Dt}$ is the rate at which heat is added to a unit mass of fluid by processes other than the release of latent heat. $\frac{D}{Dt}$ is again the substantial time derivative. The remaining symbols have been defined earlier.

DH/Dt is composed of at least two parts: (1) the convergence (or divergence) of the vertical heat flux produced by eddy motions of various scales, and (2) radiational cooling. One cannot escape the conclusion that the eddy heat flux, within the inflow layer, is convergent. The ocean supplies the atmosphere with vast amounts of sensible heat. This heat must be transported upward; it is difficult to imagine that the entire supply escapes to the upper troposphere and that none is retained by the air within the inflow layer. Furthermore, if the eddy heat transport takes place by an Austausch type mechanism, the heat flux, for saturated motions, will be toward lower values of equivalent potential temperature (θ_E). The flux will likely be convergent when $\partial^2 \theta_E / \partial z^2$ is positive. Jordan's mean tropical atmosphere [11] shows $\partial^2 \theta_E / \partial z^2$ to be positive up to at least 700 mb. There is also evidence [6] that the same type of θ_E distribution is to be found in hurricane circulations.

We now expand Dp/Dt of (38) and use the hydrostatic equation to eliminate $(1/\rho)(\partial p/\partial z)$. The result so obtained is

$$\frac{DH}{Dt} = c_p \frac{DT}{Dt} - \frac{1}{\rho} v_r \frac{\partial p}{\partial r} + gw + L \frac{Dq_s}{Dt} \quad (38a)$$

which will be useful at a later point.

By use of

$$q_s \approx \frac{\epsilon e_s}{p}, \quad (39)$$

we obtain

$$\frac{Dq_s}{Dt} = \frac{\epsilon}{p} \frac{de_s}{dT} \frac{DT}{Dt} - \left(\frac{\epsilon e_s}{RTp} \right) \frac{1}{\rho} \frac{Dp}{Dt}. \quad (40)$$

The Clausius-Clapeyron equation may be written

$$\frac{de_s}{dT} = \frac{\epsilon L e_s}{RT^2} \quad (41)$$

Combination of equations (38), (39), (40), and (41) yields

$$\frac{DH}{Dt} = \left[c_p + \frac{L^2 \epsilon^2 e_s}{R T^2 p} \right] \frac{DT}{Dt} - \left[1 + \frac{\epsilon e_s L}{R T p} \right] \left(\frac{1}{\rho} \frac{Dp}{Dt} \right). \quad (42)$$

We now eliminate $\left[1 + \frac{\epsilon e_s L}{R T p} \right]$ between (42) and (37) and obtain

$$\frac{DH}{Dt} = \left[c_p + \frac{L^2 \epsilon^2 e_s}{R T^2 p} \right] \left[\frac{DT}{Dt} - \frac{\Gamma_s}{g} \left(\frac{1}{\rho} \frac{Dp}{Dt} \right) \right] \quad (43)$$

Expansion of DT/Dt and Dp/Dt and utilization of the hydrostatic equation gives (44).

$$\frac{DH}{Dt} = \left[c_p + \frac{L^2 \epsilon^2 e_s}{R T^2 p} \right] \left\{ v_r \left(\frac{\partial T}{\partial r} - \frac{\Gamma_s}{g} \frac{1}{\rho} \frac{\partial p}{\partial r} \right) + w (\Gamma_s - \delta) \right\} \quad (44)$$

$\partial T/\partial z$ has been replaced by $-\delta$. Next, the radial gradient of temperature is eliminated between (35) and (44). The result of this operation is

$$\frac{DH}{Dt} = \frac{1}{g} \left[c_p + \frac{L^2 \epsilon^2 e_s}{R T^2 p} \right] \left\{ v_r T \left[\frac{\partial v_\theta}{\partial z} \left(f + \frac{2v_\theta}{r} \right) + \frac{\partial}{\partial z} \left(\frac{1}{\rho} \frac{\partial \tau_{rz}}{\partial z} \right) \right] + (\Gamma_s - \delta) [wg - v_r \left(\frac{1}{\rho} \frac{\partial p}{\partial r} \right)] \right\} \quad (45)$$

As we have already noted, the lapse rate above the cloud bases of the inflow layer is very nearly equal to Γ_s . If we assume this relationship to be satisfied exactly ($\delta = \Gamma_s$), equation (45) gives $DH/Dt > 0$ because $\partial v_\theta/\partial z < 0$, $v_r < 0$ and $\frac{\partial}{\partial z} \left(\frac{1}{\rho} \frac{\partial \tau_{rz}}{\partial z} \right) < 0$. Thus, air parcels above the cloud base of the inflow layer must be heated at a rate which is greater than that explicable on the basis of latent heat release ($\frac{DH}{Dt} - L \frac{Dq_s}{Dt} > -L \frac{Dq_s}{Dt}$). This is entirely consistent with the results obtained by many other authors (see, for example, [10, 15, 20, 21, 23]) from different approaches to the problem.

We now establish the fact that the $\delta = \Gamma_s$ situation is one in which the release of latent heat per unit time and mass is less than the sum of the specific kinetic energy production and the specific potential energy gain per unit time following a parcel. Above the cloud base of the inflow layer, the following inequalities are valid.

$$g w > 0 \quad (46)$$

$$-v_r \left(\frac{1}{\rho} \frac{\partial p}{\partial r} \right) > 0 \quad (47)$$

$$L D q_s / D t < 0 \quad (48)$$

$$c_p DT / Dt < 0 \quad (49)$$

From (38a), (46), (47), (48) and (49), we find the following statement to be true for the cloud region of the inflow layer.

$$\left| L \frac{Dq_s}{Dt} \right| < \left| gw - v_r \left(\frac{1}{\rho} \frac{\partial p}{\partial r} \right) \right| \quad \text{if, and only if, } \frac{DH}{Dt} > c_p \frac{DT}{Dt}. \quad (50)$$

From (45), $DH/Dt > c_p DT/Dt$ if $\delta = \Gamma_s$. Thus, from (49), $DH/Dt > c_p DT/Dt$ and, from (50), $\left| L Dq_s/Dt \right| < \left| gw - v_r \left(\frac{1}{\rho} \frac{\partial p}{\partial r} \right) \right|$.

The degree of inequality between these terms will be established in the next section. Here, however, we wish to point out that the contribution of $c_p DT/Dt$ (equation (38a)) to the maintenance of the kinetic and potential energy of a hurricane is extremely important. It is well known that the latent heat release in hurricanes is far greater than the kinetic energy production. However, this is not sufficient to explain the energy budget of inflow-layer parcels; these parcels are also gaining potential energy and, as we have just shown, $gw - v_r \left(\frac{1}{\rho} \frac{\partial p}{\partial r} \right)$ is greater than the latent heat release per unit time and mass when $\delta \approx \Gamma_s$. The needed additional supply of energy is to be found in the decrease of specific enthalpy which each inflow-layer parcel undergoes.

Thermodynamic calculations. - In this section, we will examine numerical computations, for the $\delta = \Gamma_s$ case, of several of the quantities discussed above. The term $\frac{\partial}{\partial z} \left(\frac{1}{\rho} \frac{\partial \tau_{rz}}{\partial z} \right)$ will again be neglected. Since we have already shown that this quantity is negative in the inflow layer, estimates of DH/Dt , based on (45), will be too small.

For $\delta = \Gamma_s$, equation (45), evaluated at $z = 1.75$ km., takes the approximate form

$$\frac{DH}{Dt} = \frac{T}{g} \left[c_p + \frac{L^2 \epsilon^2 e_s}{RT^2 p} \right] \left(f + \frac{2 \bar{v}_\theta}{r} \right) \bar{v}_r \frac{\partial v_\theta}{\partial z} \quad (51)$$

For computations of DH/Dt , we used \bar{v}_θ , \bar{v}_r and \bar{p} for the $I = 0.19$ case and temperatures for the $\partial v_\theta / \partial z = -1.5, -3.0, \text{ and } -4.5 \times 10^{-4} \text{ sec.}^{-1}$ cases. In addition to the computation of DH/Dt from (51), the individual terms of (38a) were calculated by means of the approximations:

$$DT/Dt = \bar{v}_r \partial T / \partial r - \delta w \quad (52)$$

$$\frac{1}{\rho} v_r \frac{\partial p}{\partial r} = (\bar{v}_r / \bar{\rho}) \frac{\partial \bar{p}}{\partial r} \quad (53)$$

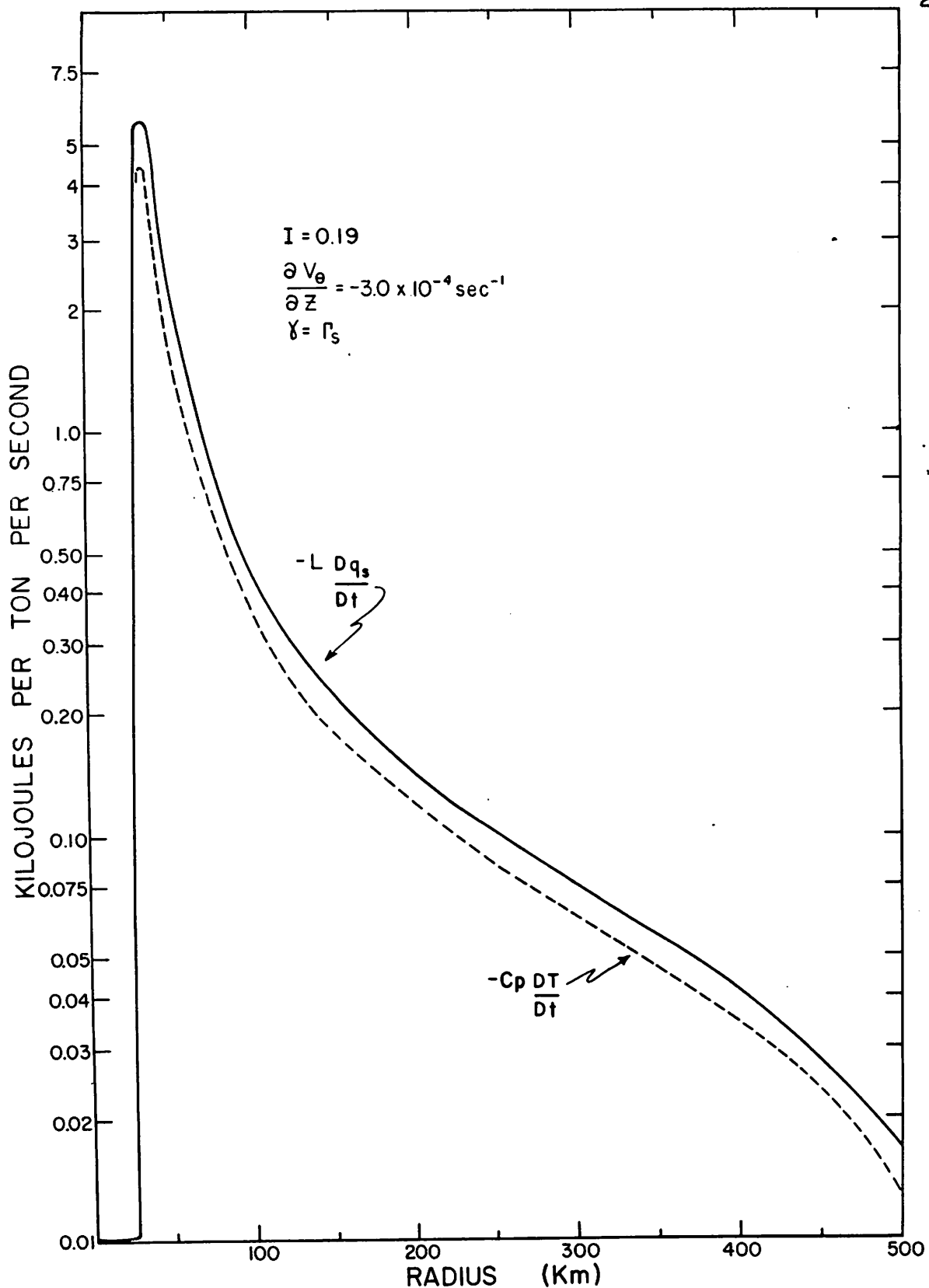


Figure 8. - Theoretical profiles of the time rates of latent heat absorption per unit mass ($-LDq_s/Dt$) and specific enthalpy change ($c_p DT/DT$) following a parcel at $z = 1.75$ km.

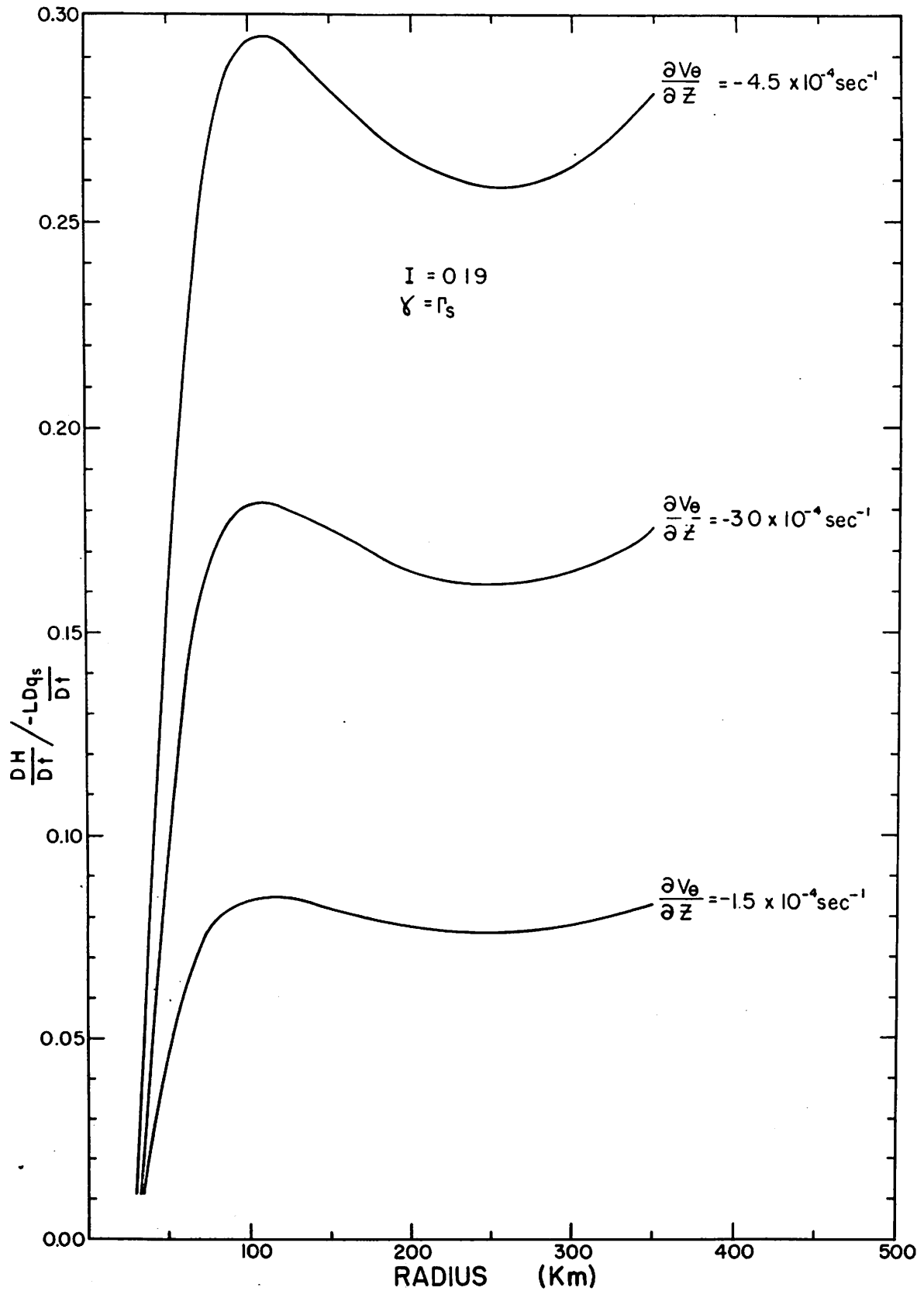


Figure 9. - Theoretical profiles of the ratio of diabatic heating (DH/Dt) to latent heat absorption ($-LDq_s/Dt$) following a unit mass of air at $z = 1.75$ km.

$$L \frac{Dq_s}{Dt} \left\{ \frac{\epsilon}{p} \frac{de_s}{dT} \frac{DT}{Dt} - \frac{\epsilon e_s}{RTp} [(\bar{v}_r/\bar{\rho}) \frac{\partial \bar{p}}{\partial r} - wg] \right\} \quad (54)$$

The vertical velocities needed for (52) and (54) were obtained as follows.

The equation of continuity can be approximated by

$$\frac{\partial(\rho w)}{\partial z} = -\rho \left(\frac{\partial v_r}{\partial r} + \frac{v_r}{r} \right). \quad (55)$$

From (13), (14) and (55), we obtain

$$\frac{\partial(\rho w)}{\partial z} = -2 \left(\frac{d\bar{v}_r}{dr} + \frac{\bar{v}_r}{r} \right) (\rho_0 + bz) \left(1 - \frac{z}{h}\right) \quad (56)$$

Integration of (56) from $z = 0$ to $z = h/2$ (1.75 km.) gives

$$w = \frac{-h \left(\frac{d\bar{v}_r}{dr} + \frac{\bar{v}_r}{r} \right) \left(\frac{3}{4} \rho_0 + b \frac{h}{6} \right)}{\bar{\rho}} \quad (57)$$

Figure 8 shows the radial distribution of $-L Dq_s/Dt$ for $\partial v_\theta/\partial z = -3 \times 10^{-4} \text{ sec.}^{-1}$. The curves for $\partial v_\theta/\partial z = -1.5 \times 10^{-4}$ and $-4.5 \times 10^{-4} \text{ sec.}^{-1}$ very nearly coincide with the one shown. Therefore, $-L Dq_s/Dt$ is primarily determined by the vertical motion and the lapse rate and is not sensitive to changes in $\partial T/\partial r$. This of course is what one would expect on intuitive grounds.

Figure 9 shows the ratio $DH/Dt / -L Dq_s/Dt$. Previous authors [20,23] have indicated that the sensible heat source is negligible with respect to the latent heat release. Figure 9 indicates that this is likely to be true in hurricanes with small vertical wind shears. For $\partial v_\theta/\partial z = -1.5 \times 10^{-4} \text{ sec.}^{-1}$, DH/Dt at $z = 1.75$ km. is less than 10 percent of $-LDq_s/Dt$ when $r < 400$ km. For $r < 50$ km., DH/Dt is less than 5 percent of $-LDq_s/Dt$. However, when $\partial v_\theta/\partial z = -4.5 \times 10^{-4} \text{ sec.}^{-1}$, DH/Dt is over 20 percent of $-LDq_s/Dt$ for $r > 60$ km. It is only within 40 km. of the storm center that $DH/Dt / -LDq_s/Dt$ becomes less than 10 percent.

Table 3 lists the distribution of the ratio

$$\frac{-(\bar{v}_r/\bar{\rho}) \frac{\partial \bar{p}}{\partial r} + gw}{-L Dq_s/Dt}$$

Table 3. - Ratio of the sum of the production rates of specific potential and specific kinetic energy to the rate of release of latent heat per unit mass of fluid following a parcel. $z = 1.75$ km., $\partial v_{\theta}/\partial z = -3 \times 10^{-4} \text{sec.}^{-1}$

Radius (km.)	$[- \bar{v}_r (\frac{1}{\rho} \frac{\partial \bar{p}}{\partial r}) + gw] / - L Dq_s / Dt$
500	2.29
450	2.11
400	2.04
350	2.01
300	2.00
250	1.99
200	1.99
150	2.00
100	2.01
90	2.00
80	1.99
70	1.97
60	1.94
50	1.90
40	1.84
35	1.81
30	1.78
27.5	1.77

for $\partial v_{\theta}/\partial z = -3 \times 10^{-4} \text{sec.}^{-1}$. Since $-LDq_s/Dt$ is not particularly sensitive to $\partial v_{\theta}/\partial z$, this table is also fairly representative of the $\partial v_{\theta}/\partial z = -1.5 \times 10^{-4}$ and $-4.5 \times 10^{-4} \text{sec.}^{-1}$ cases. Table 3 makes clear the fact that an additional energy supply, roughly as great as $-LDq_s/Dt$ is needed. From (38a), it is evident that this supply is equal to $DH/Dt - c_p DT/Dt$. We have already demonstrated that DH/Dt is much smaller than $-LDq_s/Dt$. Hence, the additional energy supply, for the most part, must be sought in the conversion of enthalpy to kinetic and potential energy. To illustrate that this is indeed the case, we have entered the $-c_p DT/Dt$ profile on figure 8 ($\partial v_{\theta}/\partial z = -3 \times 10^{-4} \text{sec.}^{-1}$). DT/Dt was obtained from (52). Figure 8 clearly illustrates the near equality of $-LDq_s/Dt$ and $-c_p DT/Dt$.

As noted in the previous section, it is well known that $-LDq_s/Dt$ is much greater than $-(\frac{v_r}{\rho} \frac{\partial p}{\partial r})$. Our results, despite table 3, are not inconsistent with this fact. Figure 10 shows separate plots of $-(\bar{v}_r/\bar{\rho}) \frac{\partial \bar{p}}{\partial r}$ and gw . Over most of the diagram, gw is 20 to 30 times the greater and it is nowhere less than 15 times larger. Hence, even though $-(\bar{v}_r/\bar{\rho}) \frac{\partial \bar{p}}{\partial r} + gw$ is greater than $-L Dq_s/Dt$

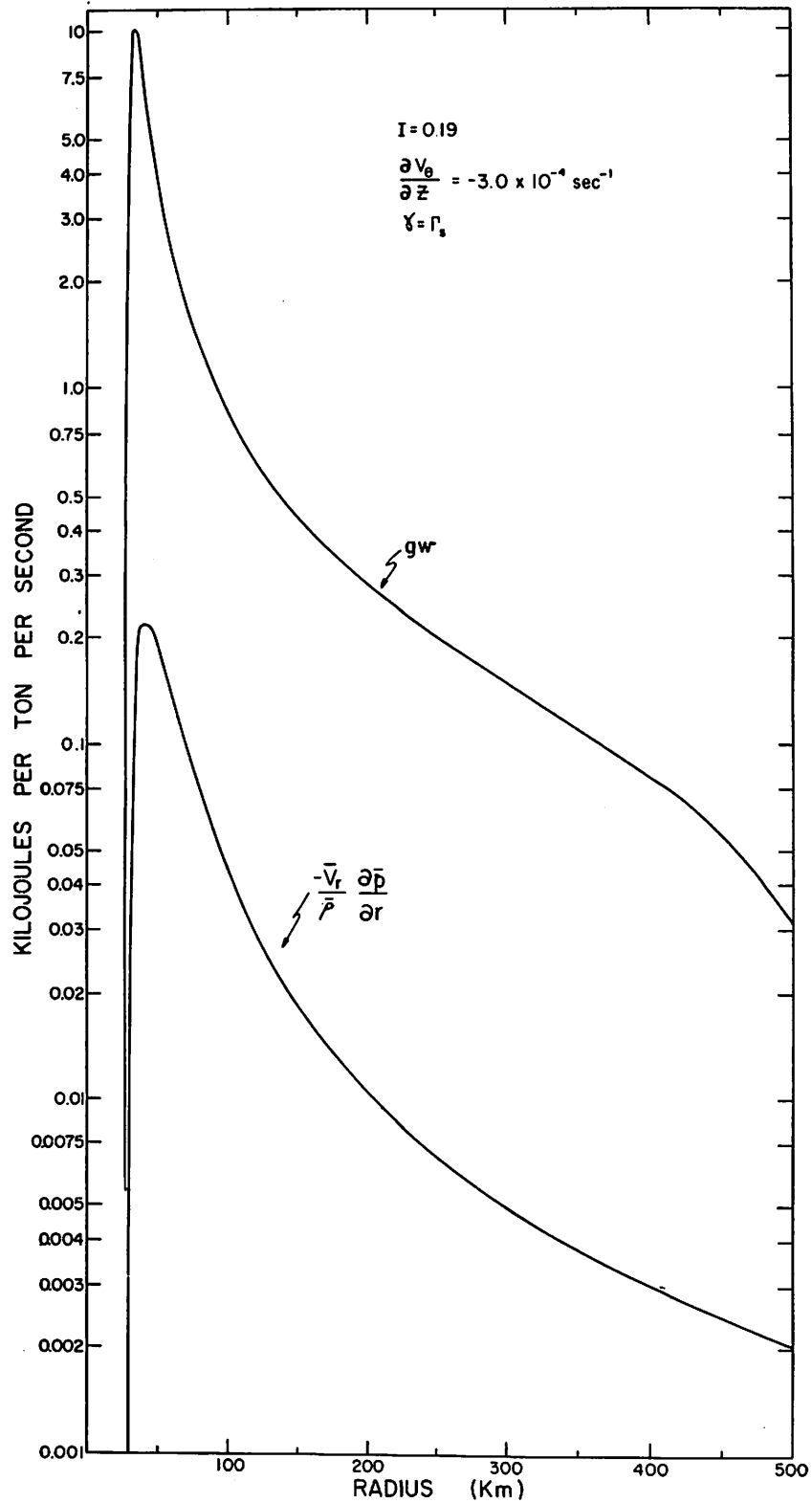


Figure 10. - Theoretical profiles of the rate of gain of specific potential energy (gw) and the per unit mass rate of production of kinetic energy ($-\frac{\bar{v}_r}{\bar{\rho}} \frac{\partial \bar{p}}{\partial r}$) following a parcel at $z = 1.75$ km.

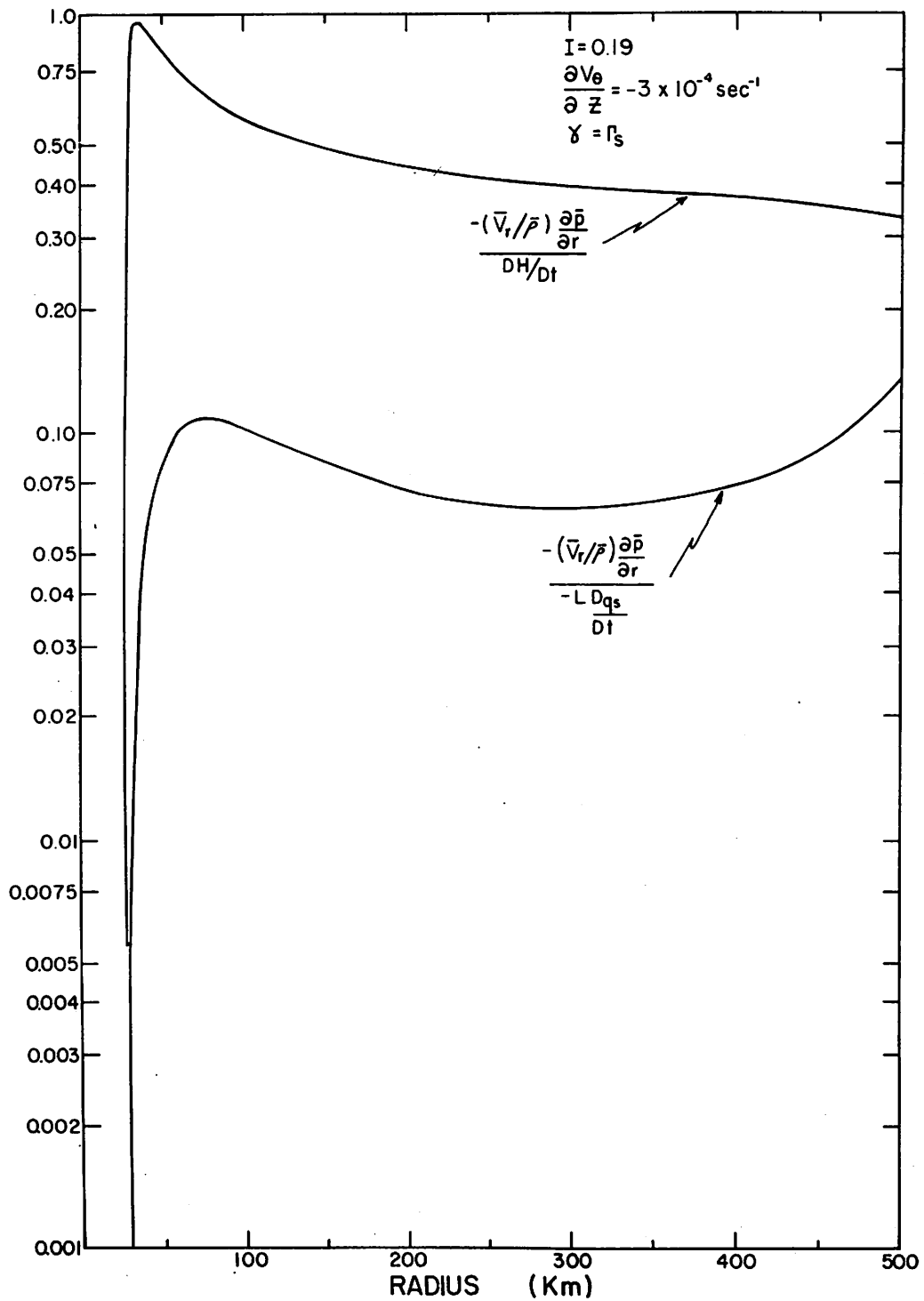


Figure 11. - Theoretical profiles of the ratio of: (1) the kinetic energy production rate to the diabatic heating rate $(-\bar{v}_r/\bar{\rho}) \frac{\partial \bar{p}}{\partial r} / \frac{DH}{Dt}$, and (2) the kinetic energy production rate to the rate of absorption of latent heat $(-\bar{v}_r/\bar{\rho}) \frac{\partial \bar{p}}{\partial r} / -L \frac{Dq_s}{Dt}$ following a parcel at $z = 1.75$ km.

by a factor of 1.8 to 2.3, $-(\bar{v}_r/\bar{\rho}) \frac{\partial \bar{p}}{\partial r}$ itself is much smaller than $-L Dq_g/Dt$. The ratios, $-(\bar{v}_r/\bar{\rho}) \frac{\partial \bar{p}}{\partial r} / (-L Dq_g/Dt)$ and $-(\bar{v}_r/\bar{p}) \frac{\partial \bar{p}}{\partial r} / DE/Dt$ are illustrated by figure 11 ($(\partial v_\theta/\partial z) = -3 \times 10^{-4} \text{ sec.}^{-1}$). For most radii, kinetic energy production is less than 1/10 of the latent heat release. Within 50 km. of the storm center, this ratio decreases to very small values.

Palmén [21] has estimated that, within 220 km. of the storm center, kinetic energy production is only 3 percent of latent heat release. This figure, however, represents the integrated effect for the entire troposphere and has little significance with respect to individual air parcels of the inflow layer. The outflow in the upper troposphere is a process which consumes kinetic energy (flow toward higher pressure) and since latent heat is released in significant amounts up to at least 300 mb., the ratio of the vertical integrals of kinetic energy production and latent heat release should be much smaller than the ratio of these terms for an individual air parcel in the inflow layer.

4. SUMMARY AND CONCLUSIONS

It is a fairly simple matter to extend the Malkus-Riehl model of the hurricane-inflow layer to include vertical variations of density and radial velocity. The solutions obtained for the tangential velocity and the vertically integrated pressure are realistic to the point that they may be used as a posteriori evidence to justify the assumed relationship between \bar{v}_θ and \bar{v}_r . It would also appear that the values employed for the various parameters are essentially correct.

The thermodynamic relationships which are implied by the model velocity and pressure fields were examined. It was found that air parcels within the inflow layer must be heated at a rate which exceeds that possible when latent heat release is the sole heating mechanism. This is in agreement with the results obtained by several authors from arguments which differ from those used here. The magnitude of this heating depends, for pseudoadiabatic lapse rates, mainly upon the vertical wind shear. With relatively small wind shears, the additional heating is less than 10 percent of the latent heat release. However, for storms with fairly large wind shears, the additional heating approaches a radial average which exceeds 25 percent of the latent heat release.

Although the latent heat release is much larger than the kinetic energy production, the sum of the specific potential energy gain plus the specific kinetic energy production per unit time, following an air parcel, is 1.8 to 2.3 times greater than the rate at which these parcels absorb released latent heat. The additional energy needed to provide an energy balance for each parcel is supplied, for the most part, by the conversion of specific enthalpy to potential and kinetic energy.

ACKNOWLEDGMENTS

The author is indebted to Miss Noreen Brady, formerly of the National Hurricane Research Project staff, for the machine coding of numerous computa-

tions. Mrs. Bonnie True typed the manuscript. Mr. Robert Carrodus and Mr. Charles True were responsible for reproducing the figures.

REFERENCES

1. W. Blumen and N. E. LaSeur, "Some Details of the Wind Field in Individual Hurricanes," Florida State University, Scientific Report No. 7 under Contracts AF19(604)-753(GRD) and Cwb-9121(USWB), 1958, 45 pp.
2. J. A. Colón, "The Structure of Hurricane Daisy, 1958," to be issued in NHRP report series.
3. E. L. Deacon, P. A. Sheppard, and E. K. Webb, "Wind Profiles over the Sea and the Drag at the Sea Surface," Australian Journal of Physics, vol. 9, No. 4, Dec. 1956, pp. 511-541.
4. V. W. Ekman, "On the Influence of the Earth's Rotation on Ocean Currents," Arkiv Mat. Astr. Fys. vol. 2, No. 11, 1905, 52 pp.
5. R. D. Fletcher, "Computation of Maximum Surface Winds in Hurricanes," Bulletin of the American Meteorological Society, vol. 36, No. 6, June 1955, pp. 247-250.
6. M. Gangopadhyaya and H. Riehl, "Exchange of Heat, Moisture, and Momentum Between Hurricane Ella (1958) and Its Environment," National Hurricane Research Project Report No. 29, 1959, 12 pp.
7. S. L. Hess, Introduction to Theoretical Meteorology, Henry Holt, New York, 1959, 362 pp.
8. L. A. Hughes, "On the Low-Level Wind Structure of Tropical Storms," Journal of Meteorology, vol. 9, No. 6, Dec. 1952, pp. 422-428.
9. E. S. Jordan, "An Observational Study of the Upper Wind-Circulation Around Tropical Storms," Journal of Meteorology, vol. 9, No. 5, Oct. 1952, pp. 340-346.
10. C. L. Jordan and E. S. Jordan, "On the Mean Thermal Structure of Tropical Cyclones," Journal of Meteorology, vol. 11, No. 6, Dec. 1954, pp. 440-448.
11. C. L. Jordan, "Mean Soundings for the Gulf of Mexico Area," National Hurricane Research Project Report No. 30, 1959, 10 pp.
12. N. E. LaSeur, "An Analysis of Some Detailed Data Obtained by Aircraft Reconnaissance of a Hurricane," Florida State University, Scientific Report No. 5, under Contracts AF19(604)-753(GRD) and Cwb-8822 and Cwb-9121(USWB), 1957, 25 pp.
13. N. E. LaSeur, Final Report under Contract AF19(604)-753, Florida State University, 1959.
14. J. S. Malkus, "On the Thermal Structure of the Hurricane Core," Proceedings Technical Conference on Hurricanes, Nov. 19-22, 1958, Miami Beach, Fla. American Meteorological Society, 1958, Sec. D.3. (abstract).
15. J. S. Malkus and H. Riehl, "On the Dynamics and Energy Transformations in Steady-State Hurricanes," National Hurricane Research Project Report No. 31, 1959, 31 pp.
16. B. I. Miller, "The Three-Dimensional Wind Structure Around a Tropical Cyclone," National Hurricane Research Project Report No. 15, 1958, 41 pp.
17. W. E. Milne, Numerical Solution of Differential Equations, Wiley and Sons, New York, 1953, 275 pp.
18. E. Palmén and L. Laurila, "Über die Einwirkung eines Sturmes auf den Hydrographischen Zustand in Nördlichen Ostseegebiet," Societas Scientiarum Fennica, Commentationes Physica - Mathematicae, vol. 10, No. 1, 1938, 53 pp.

19. E. Palmén and H. Riehl, "Budget of Angular Momentum and Energy in Tropical Cyclones," Journal of Meteorology, vol. 14, No. 2, Apr. 1957, pp. 150-159.
20. E. Palmén, "Energy Problems of the Tropical Hurricanes," Proceedings Technical Conference on Hurricanes, Nov. 19-22, 1958, Miami Beach, Fla. American Meteorological Society, 1958, Sec. C.11.
21. C.H.B. Priestley, Turbulent Transfer in the Lower Atmosphere, University of Chicago Press, Chicago, 1959, 130 pp.
22. H. Riehl, Tropical Meteorology, McGraw-Hill Book Co., Inc., New York, 1954, 392 pp.
23. H. Riehl and J. S. Malkus, "Some Aspects of Hurricane Daisy, 1958," National Hurricane Research Project Report No. 46, 1961, 64 pp.
24. H. U. Sverdrup, "Oceanography," pp. 608-670 in Handbuch der Physik, Band XLVIII, Geophysik II, Springer-Verlag, Berlin, 1957.